We are IntechOpen,
the world's leading publisher of Open Access books
Built by scientists, for scientists

6,900
Open access books available

186,000
International authors and editors

200M
Downloads

154
Countries delivered to

Our authors are among the

TOP 1%
most cited scientists

12.2%
Contributors from top 500 universities

WEB OF SCIENCE™

Selection of our books indexed in the Book Citation Index
in Web of Science™ Core Collection (BKCI)

Interested in publishing with us?
Contact book.department@intechopen.com

Numbers displayed above are based on latest data collected.
For more information visit www.intechopen.com

Polymer Coated Rayleigh SAW and STW Resonators for Gas Sensor Applications

Ivan D. Avramov
Georgi Nadjakov Institute of Solid State Physics, Sofia
Bulgaria

1. Introduction

Polymer coated gas-phase sensors using the classical Rayleigh-type surface acoustic wave (RSAW) mode have enjoyed considerable interest worldwide over the last two decades [1-3]. This interest is motivated by their orders of magnitude higher sensitivity and larger dynamic range compared to bulk acoustic wave (BAW) sensors, fast response times, excellent overall stability, coming close to that of quartz crystal sensors, and low phase noise of the sensor system making high-resolution measurements possible [4]. Because of these features that are difficult to achieve with other technologies, RSAW based gas sensors have found successful application in a variety of industrial implementations such as electronic noses, systems for analysis of chemical and biological gases, medical diagnostics, environmental monitoring and protection, etc. [5-11]. On the other hand, surface transverse wave (STW) based gas sensors, even though sharing the same operation principle, have not been studied so extensively yet. The purpose of this article is to present and discuss systematic experimental data with both acoustic wave modes which will prove that STW based gas-phase sensors not only successfully compete with their RSAW counterparts but also complement them in applications where RSAW gas sensors reach their limits. Successful corrosion proof RSAW sensors using gold metallization for operation in highly reactive chemical environments will also be presented.

2. Operation principle of RSAW/STW based resonant gas phase sensors

Both RSAW and STW based gas sensitive resonant sensors share the same operation principle illustrated in Fig. 1. The sensor device typically is a two-port RSAW or STW resonator on a temperature compensated rotated Y cut of quartz whose geometry has been optimized in such manner that the resonator retains a well behaved single-mode resonance and suffers minimum loss increase and Q-degradation after the gas sensitive layer, (typically a solid, semisolid or soft polymer film with good sorption properties), is deposited on its surface. On the other hand, the sensor has to have maximum active area in the centre of its geometry where the magnitude of the standing wave and deformation are maximized. Thus, strong interaction with the gas adsorbed in the polymer film occurs and maximum gas sensitivity is obtained. The sensor operation principle according to Fig. 1 is fairly simple. If a gas-phase analyte of a certain concentration is applied to its surface, gas molecules are absorbed by the sensing layer until thermodynamic equilibrium is achieved; i. e. the number

of adsorbed molecules becomes equal to the number of desorbed ones. Due to adsorption, the layer becomes heavier and this increases the mass loading on the sensor surface. As a result of that, the acoustic wave propagation velocity v decreases and causes a concentration proportional frequency down shift Δf of the sensor's resonance, called sensor signal. The resonance frequency shift of RSAW gas sensors coated with a polyisobutilene (PIB) polymer film is shown in Fig. 2 a) and b) for two different concentrations of tetrachloroethilene vapors. If the vapor concentration is small (0,1% in Fig. 2 a)) then the resonance shifts down by 83 ppm without degradation in loss or Q. At large concentrations of the gas vapors (0,7% in Fig. 2 b)), the 550 ppm of observed frequency down shift is accompanied by a 2 dB loss increase due to the heavy mass loading. However, the sensor device retains a high loaded Q, (above 2000 in Fig. 2 a) versus >4000 in Fig. 2 b)) and a steep phase slope in a well behaved single-mode resonance without distortion or excitation of undesired longitudinal modes.
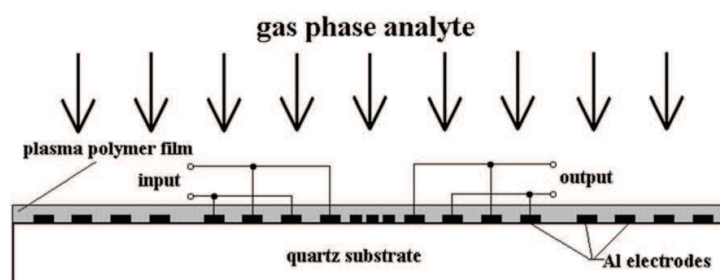

Fig. 1. Operation principle of RSAW/STW based resonant gas phase sensors
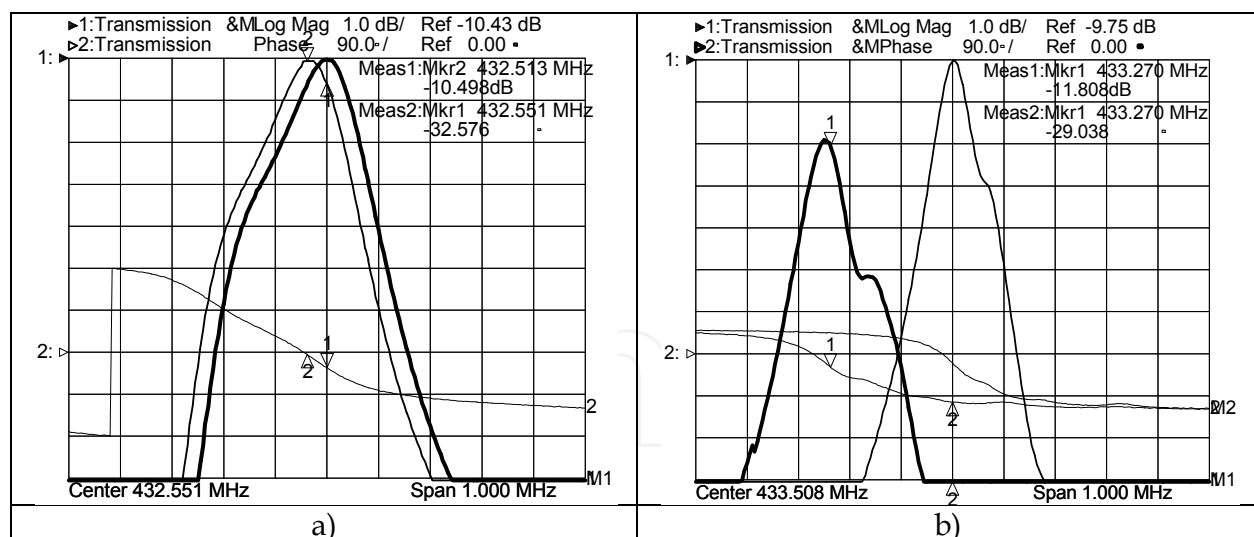
Fig. 2. Frequency (upper curves and phase (lower curves) responses of PIB coated RSAW sensors prior to (right) and after (left) tetrachloroethilene vapor probing at a) 0,1% and b) 0,7% concentration

3. Measurement resolution of RSAW/STW gas phase sensor systems

If a sensor device as the ones from Fig. 2 a) and b) is used as a frequency stabilizing element in the feedback loop of an oscillator circuit and its frequency f_0 is adjusted at the resonance

frequency of the sensor (see marker positions in Fig. 2 a) and b)) then due to the high Q of the sensor device, low-noise oscillation with high short-term stability will be obtained. Any change in gas concentration will alter the resonance frequency and the output frequency f_0 of the sensor oscillator, accordingly. Thus Δf can be measured with a high precision using a high-resolution frequency counter, connected to the output of the sensor oscillator. At a given gas concentration C, measured in parts per million (ppm), the resolution R of the sensor system, also measured in ppm, will be limited only by the short-term stability of the sensor oscillator $\sigma_y(\tau)$, also called Allan's variation, for the measurement time τ. *The value of $\sigma_y(\tau)$ represents the flicker phase noise of the sensor oscillator in the time domain which is dominated by the actual flicker phase noise of the coated acoustic wave sensor.* The resolution R determines the minimum change in gas concentration that the system can detect and is, therefore, also called detection limit. It is calculated as follows:

$$R = [C\sigma_y(\tau)f_0\tau] / \Delta f \tag{1}$$

To calculate R for a given gas concentration C, according to (1), it is sufficient to measure $\sigma_y(\tau)$ of the sensor oscillator for the time interval τ which is normally 1s for most frequency counters operating in the typical 0,3 to 1,0 GHz RSAW/STW sensor range with 1 Hz resolution. Then, according to [12], $\sigma_y(\tau)$ can be calculated from a finite number M of consecutive frequency measurements y_i of f_0 as:

$$\sigma_y(\tau) = \left[\frac{1}{2(M-1)} \sum_{i=1}^{M-1} (y_{i+1} - y_i)^2 \right]^{1/2} , \tag{2}$$

where i is an integer. In a well stabilized against thermal transients sensor oscillator typically 20 to 50 consecutive measurements of f_0 are enough to calculate $\sigma_y(\tau)$ with sufficient accuracy for practical sensor applications.

4. Chemosensitive layers for RSAW/STW based gas sensors

The correct choice of the sensing layer suitable for the chosen acoustic mode is the key to proper sensor operation and good sensitivity and dynamic range [13, 14]. A sensing layer is considered as "good" if it has an excellent adhesion to the surface of the acoustic device for proper interaction with the acoustic wave, can easily adsorb and restlessly desorb large amounts of probing gases without chemically reacting with them, has good temperature stability and low ageing and does not change its sensitivity and sorption characteristics over thousands of measurement cycles. It is also desirable that the layer provides some selectivity to a certain chemical compound, i. e. it absorbs larger amounts of that compound than other compounds. Finally, the layer should not significantly degrade the Q, loss and the shape of the resonance after deposition onto the acoustic device.

Because of their complicated net structure, many polymers feature excellent physical sorption, as required for reproducible sensor performance and this makes them appropriate for gas sensing applications [15-19]. If some of them have also appropriate viscoelastic properties for good interaction with the RSAW or STW mode, then they will provide the required performance of the acoustic wave sensor, accordingly. Layers with appropriate viscoelastic properties are those that follow the deformation of the surface as a result of the wave propagation without causing significant propagation loss and conversion of the

acoustic energy into undesired modes that decay into the bulk of the substrate and may cause degradation of sensor performance.

An important parameter of the sensing film, except for its viscoelastic properties is its solidness. On one hand, the parameter "solidness" determines the sorption properties of the film and the amount of gas that the layer can accommodate before saturation is reached. On the other hand, it determines the way in which the polymer film interacts with the acoustic wave. Therefore, the film solidness will determine the sensitivity, dynamic range and detection limit of the sensor. Based on their solidness, there are three types of polymer films that are appropriate for RSAW/STW sensors:

a. *Solid polymer films*. In fact, these films are solid as glass. That is why, they are often called "glassy polymer films" and have a stiffness value close to that of the sensor's quartz substrate that they are deposited on. If used with the STW mode, due to the lower propagation velocity, these solid films trap the wave energy to the substrate surface and the acoustic wave propagates with low loss. That is why, solid films work much better with the STW mode than with the RSAW one. When their thickness becomes too high, a second slightly faster mode, called "Love mode" gets excited and multimoding occurs. Solid polymer films feature surface sorption and become easily saturated by the adsorbed gas but on the other hand, they feature very fast response times and are very sensitive if the sensor is operated far below saturation. That is why they are appropriate for high resolution measurements at low gas concentrations, (typically below 0,1%). A typical representative of the solid polymer family is the hexamethyldissiloxane (HMDSO), obtained in a glow-discharge plasma polymerization process [19].

b. *Soft polymer films*. These films are soft and elastic just like rubber. That is why they are referred to as "rubbery" or "jelly-like" films. Typically, they are deposited using spin coating or more advanced techniques such as airbrush or electro spray methods that provide good control over film thickness and uniformity. Since these soft polymers provide profound bulk sorption, they are capable of adsorbing large amounts of gas and are appropriate for measurements at high gas concentrations, (typically above 0,1%). They are well tolerated by the RSAW mode but do not work so well with STW. The reason is that they cause energy leakage of the STW into the bulk of the soft layer which results in increased loss and Q-degradation of the sensor resonator. Polymers like polyisobutilene (PIB), poly-(2-hydroxyethylmethacrylate) (PHEMA) and poly-(n-butylmethacrylate) (PBMA) are often used in RSAW based gas sensors.

c. *Semisolid polymer films*. These light and highly elastic films are also typically obtained in a plasma polymerization process [17, 18] for good reproducibility of the film parameters and have a structure very similar to polystyrene, the material used in plastic bags. They are highly resistant to almost all aggressive chemicals such as acids, bases and organic solvents and this makes them appropriate for environmental sensing applications. They are well tolerated by both, the RSAW and STW mode and often feature sensitivities comparable to those of the soft polymer films. The two semisolid films used in this study are styrene (ST) and allylalkohol (AA) synthesized in a plasma polymerization reactor.

5. Comparative characteristics of polymer coated RSAW and STW gas sensors operating at the same acoustic wave length

To identify the advantages and disadvantages of the STW mode versus its RSAW counterpart on quartz for gas sensor applications it is necessary to compare the sensor

performance of both modes under identical real-life conditions. Such a performance comparison would be correct only if it is carried out with sensor devices of both modes operating on the same acoustic wave length for the following reason: If both types of devices are fabricated on the same piezoelectric material and cut orientation (AT-cut quartz in this case), use the same device geometry, are coated with the same sensing layer of the same thickness and are probed with identical gases and concentrations, then the only factors responsible for the differences in electrical and sensor performance would be the type of motion for each mode, (elliptical for the RSAW and shear horizontal for the STW) and the way the acoustic wave interacts with the sensing layer. The results presented in the next sections were performed with RSAW and STW sensors whose electrical characteristics in the uncoated state are summarized in Table 1.

5.1 Electrical performance of STW/RSAW sensor resonators coated with solid and semisolid sensing layers

The frequency and phase responses of the STW and RSAW sensor resonators from Table 1 prior to and after coating with the solid HMDSO are compared in Fig. 3. After film deposition, the frequency of the RSAW device shifts down by about 1,5 MHz (3500 ppm), its insertion loss increases by 5,7 dB and the loaded Q decreases from 6000 to about 2000.

Acoustic wave mode	STW	RSAW
Acoustic wave length	7,22 μm	7,22 μm
Sensor resonator frequency	433 MHz	701 MHz
Device insertion loss	5-7 dB	6-7 dB
Loaded Q-factor	3000-4000	5000-6000
Side lobe suppression	> 8 dB	>12 dB
Metallisation	Al	Al

Table 1. Electrical characteristics of the uncoated STW/RSAW sensor resonators used in the comparative studies

In addition, the RSAW device retains a well behaved single-mode resonance with excellent side lobe suppression as required for stable operation of the sensor oscillator. The STW device shows a different behavior. Its frequency shifts down by 4 MHz (6100 ppm) which accounts for about 2 times higher relative mass loading sensitivity than its RSAW counterpart. The insertion loss increases by just about 3 dB versus 5,7 dB for the RSAW mode which implies that the STW mode tolerates solid films better in terms of loss increase. On the other hand, excitation of a second higher-order Love wave mode [20] about 7 MHz higher than the main STW mode at 697 MHz is observed. Since a 180 deg. phase reversal at this Love mode occurs, (see the lower data plot in Fig. 3 b)), it is not very likely to degrade the performance of the sensor oscillator. A more serious problem, however, is the distortion at the main STW mode that indeed can cause the sensor oscillator to jump onto an adjacent peak during the measurement. That is why, coating STW sensor resonators with excessively thick solid films as the 190 nm HMDSO from Fig. 3 should be stopped before distortion and multiple peak behavior on the main STW mode occurs. As far as the higher-order Love mode at 704 MHz is concerned, we have noticed that its gas sensitivity is orders of magnitude lower than the STW mode on the right side. This lack of sensitivity is explained by the fact that the Love mode scatters its energy into the bulk of the sensing layer [20].
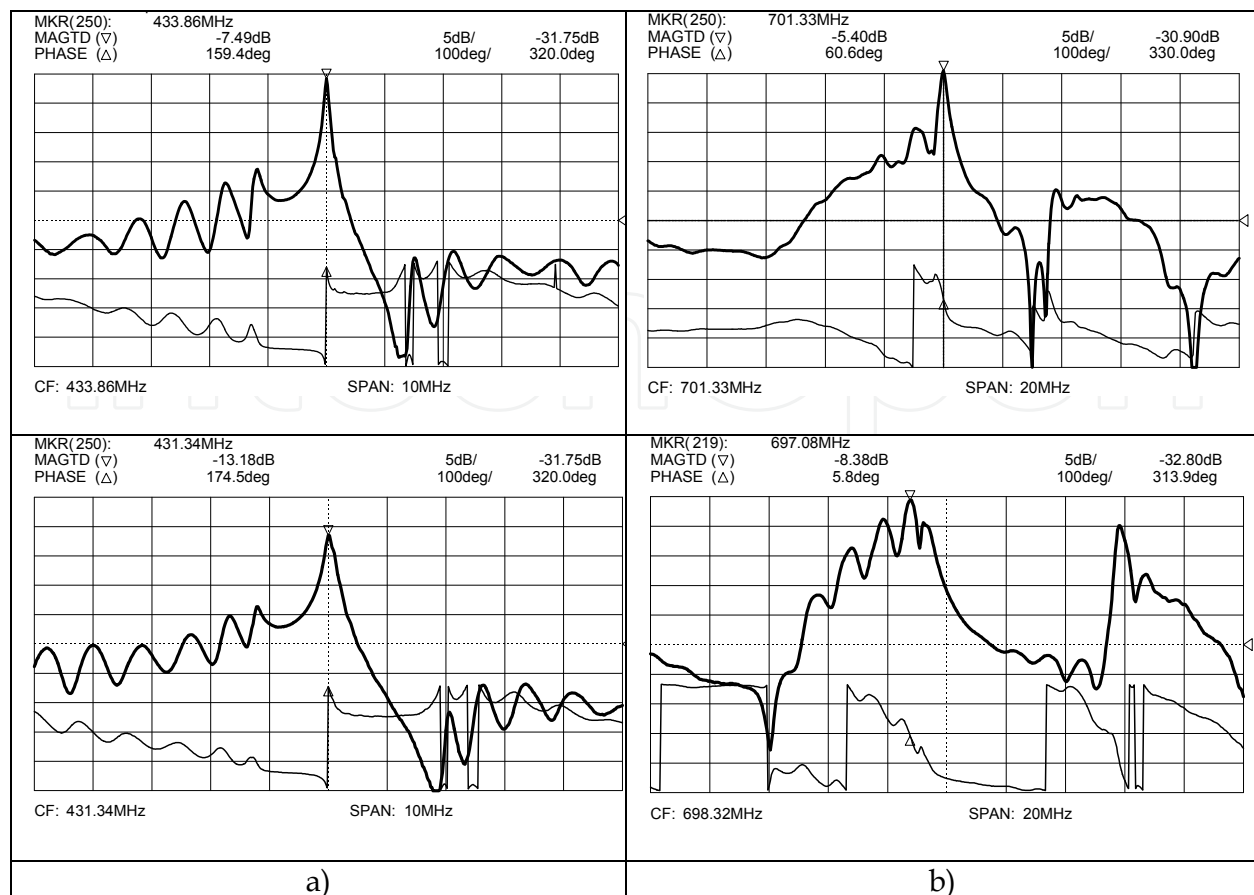
Fig. 3. Frequency (upper curves) and phase responses (lower curves) of the a) RSAW and b) STW sensor resonators from Table 1 prior to (upper plots) and after (lower plots) 190 nm HMDSO solid film deposition

5.2 Electrical performance of STW/RSAW sensor resonators coated with soft polymer films

A similar comparison between both acoustic wave modes was performed by coating the devices from Table 1 with the soft polymer film PIB using the micro drop deposition method. The data obtained shows quite the opposite tendency compared to the solid film behavior from Section 5.1. The STW devices suffered a 5 dB increase in insertion loss and rather distorted frequency responses even at fairly thin soft layers. Only a moderate frequency down shift of 1330 ppm was obtain as a result of film coating. As evident from the frequency responses in Fig. 2 the RSAW devices were found to provide a much better performance at the same film thickness. They retain a high loaded Q and low insertion loss, as well as an undistorted single-mode resonance. These data imply that RSAW sensors will work better with soft polymer films while the STW mode will provide better performance with solid films as long as they are not excessively thick to cause distortion.

6. A practical method for film thickness optimization of RSAW/STW gas sensors coated with solid and semisolid sensing layers

The most important step in designing practical RSAW/STW resonant sensors is the selection of an optimum thickness of the sensing layer. It should be selected in such manner

that maximum sensor sensitivity and dynamic range are obtained at minimum degradation of the electrical resonator performance (insertion loss, loaded Q, side lobe suppression and distortion) as required for stable low-noise operation of the sensor oscillator. A very efficient method for film thickness optimization using a controlled plasma deposition of the semisolid polymer Parylene C is described in [21]. This material has viscoelastic properties very similar to practical solid and semisolid layers but has the unique feature that it can polymerize directly on the surface of the acoustic devices at room temperature, thus avoiding undesired thermal frequency drifts. Also the actual deposition is performed in a chamber separate from the plasma reactor where the devices are protected from the high electric fields of the main plasma generator. This allows direct measurement of their frequency and phase responses with a network analyzer in the process of film deposition while the film thickness is measured with a quartz crystal microbalance (QCM). The results from a Parylene C deposition on a 433 MHz RSAW resonator and real time measurements of its electrical characteristics are shown in Fig. 4 for a polymer thickness ranging from 0 to 700 nm. From this measurement it is possible to identify the thickness range in which optimum sensor performance is expected and to extract information on the behavior of important sensor parameters in the process of polymer coating as follows:

• the down shift of the resonant frequency versus film thickness;
• the loss increase with film thickness;
• the loaded Q decrease with film thickness;
• the behavior of the adjacent longitudinal modes in the process of deposition;
• the thickness range over which the sensor demonstrates maximum mass sensitivity of frequency while retaining good electrical performance. In Fig. 4 this optimum thickness range is between 100 and 300 nm with an average of 200 nm.
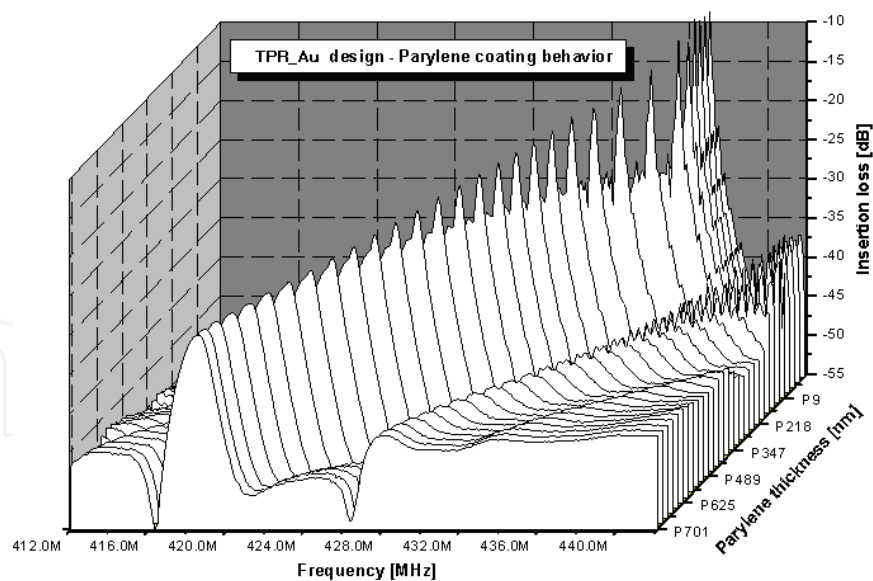

Fig. 4. Parylene C coating behavior of a 433 MHz RSAW sensor resonator in the 0 to 700 nm polymer thickness range

As evident from Fig. 4, in the optimum thickness range (100 to 300 nm) a maximum linear frequency shift, (maximum mass sensitivity), is accompanied by just about 7 dB loss increase. The Q remains high as shown by the sharp resonance while the first longitudinal mode on the left side of the resonance remains suppressed by at least 12 dB. If the sensor is

intended for high-resolution measurements at low gas concentrations, then a thickness close to 100 nm should be chosen due to the highest Q and lowest loss. If measurements at higher gas concentrations are expected then a 300 nm thickness may be more appropriate since the thicker layer may adsorb larger amounts of gas without film saturation.

6.1 Critical thickness in RSAW/STW based sensor resonators coated with solid and semisolid sensing layers

As shown in the previous sections, the sensing layer does not only shift the resonant frequency down, increase the loss and decrease the loaded Q as a result of mass loading but it also influences the longitudinal modes supported by the resonator geometry that appear on the left side of the main resonance. In the uncoated resonator these modes are well enough suppressed (typically by 5 to 15 dB) and do not cause any problems when the resonator is operated in an oscillator circuit. As soon as a sensing layer is deposited on the surface, it will change the phase conditions along the device topology and this will cause the adjacent longitudinal modes to arise in magnitude at the expense of the main resonance. This situation gets worse at thick solid films for both, the STW and the RSAW mode. At a certain thickness which we call "critical thickness" the magnitude of the first adjacent low-frequency longitudinal mode on the left becomes equal to the magnitude of the higher-frequency main resonance. This creates a potential for instability in the sensor oscillator stabilized with this sensor since it can easily jump from the main resonance onto the left longitudinal mode during gas probing which will ruin the measurement. The critical thickness situation is illustrated in Fig. 5 a) and b) for a STW and a RSAW device from Table 1, accordingly, in the process of Parylene C deposition as described in Section 6. As evident from Fig. 5 a), at thickness values above 185 nm the first longitudinal mode on the left starts rapidly growing until its magnitude becomes equal to the main resonance. The critical thickness at which this happens is about 350 nm. At this thickness also a strong Love mode excitation on the right is observed. The RSAW device in Fig. 5 b) reaches its critical thickness at about 650 nm. From these data we can draw the conclusion that the devices from Table 1 can be usable as Parylene C coated sensors as long the film thickness is lower than 300 nm and 600 nm for the STW and RSAW devices, respectively. Comparing the coating behavior of both modes in Fig. 5 we see that the STW mode retains a much better behaved resonance than its RSAW counterpart until the critical thickness is reached. At that thickness the STW device has a loss of 14 dB (Fig. 5 a)), versus 35 dB for the RSAW device (Fig. 5 b)). Therefore, the STW mode tolerates solid and semisolid sensing films much better than the RSAW one and is more appropriate for operation with such films in practical gas sensors.

7. Gas sensing characteristics of RSAW/STW resonant sensors coated with solid and semisolid chemo sensitive films

In the following sections we present results from gas probing experiments on RSAW/STW sensors coated with solid HMDSO and semisolid ST and AA films. Four different chemical agents at different vapor concentrations are used for gas probing as follows:

- Dichloroethane   6500 ppm
- Ethylacetate   17600 ppm
- Tetrachloroethylene   2650 ppm
- Xylene   1400 ppm

The purpose of the gas probing tests is to identify which acoustic wave mode provides better performance in real-world gas sensing conditions.
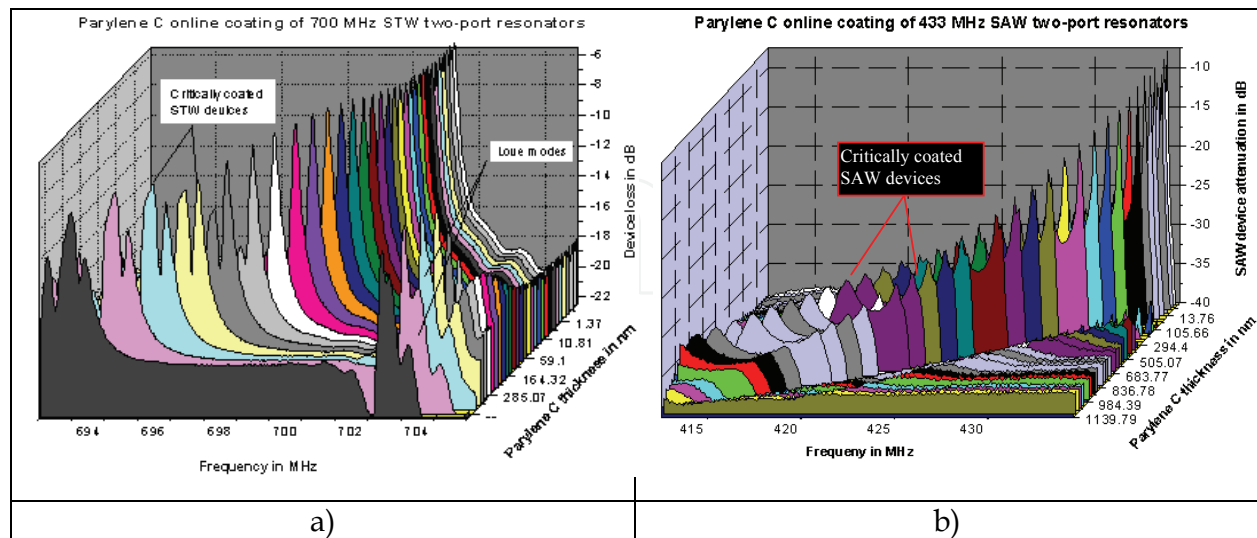

Fig. 5. Critical thickness in a) STW and b) RSAW devices in the process of Parylene C coating

7.1 Computer controlled automatic system for gas probing measurements

The block diagram of the computer controlled system for measuring the gas sensing characteristics of the RSAW/STW polymer coated sensors is shown in Fig. 6. For correct comparison of the gas probing performance of both acoustic wave modes four pairs of devices (one RSAW and one STW sensor in each pair, coated with the same polymer to the same film thickness and in the same deposition process) are mounted in open TO 92 packages and placed in the sensor head which can accommodate a total of eight sensors. Each device is connected to one of the 8 sensor oscillator circuits in the head. During gas probing each of the 8 oscillators is turned on for a short period of time to take the measurement. The oscillators are operated one at a time and multiplexed consecutively to avoid possible injection locking. Their output frequency is down converted to an intermediate frequency in the 4-9 MHz range by means of a stable heterodyne reference oscillator to allow fast high-resolution measurements with a reciprocal frequency counter. The chemical compounds 1 through 4 used for gas probing are vapors from the 4 liquid-phase analytes in the 4 containers. A permeation cell is placed on top of each container to allow a defined vapor pressure which is controlled by the rotation speed of the pump. By a switch block of valves the vapors of each analyte are then consecutively fed to the sensor head where they interact with the sensors. After the measurements at each analyte are completed the sensors are flushed with dry air passing through a silica gel integrator which provides also a homogenous air and gas flow. The entire system is controlled by a computer which performs measurements in probe-flush cycles over time and provides real-time sensor data on the computer screen. The data in Fig. 7 is the gas probing performance of a 700 MHz STW styrene coated sensor probed with dichloroethane vapors at 6500 ppm concentration in 100 s probe-flush cycles. It should be noted that prior to this measurement the sensor was probed with a different compound (xylene) for 62 hours and 40 minutes. Note the excellent reproducibility of the noise free sensor signal with a magnitude

Δf=160KHz over time indicating that prolonged xylene treatment has not had any influence on the sensor performance. This is a clear indication that styrene has very good physical sorption properties to a variety of gas phase compounds.
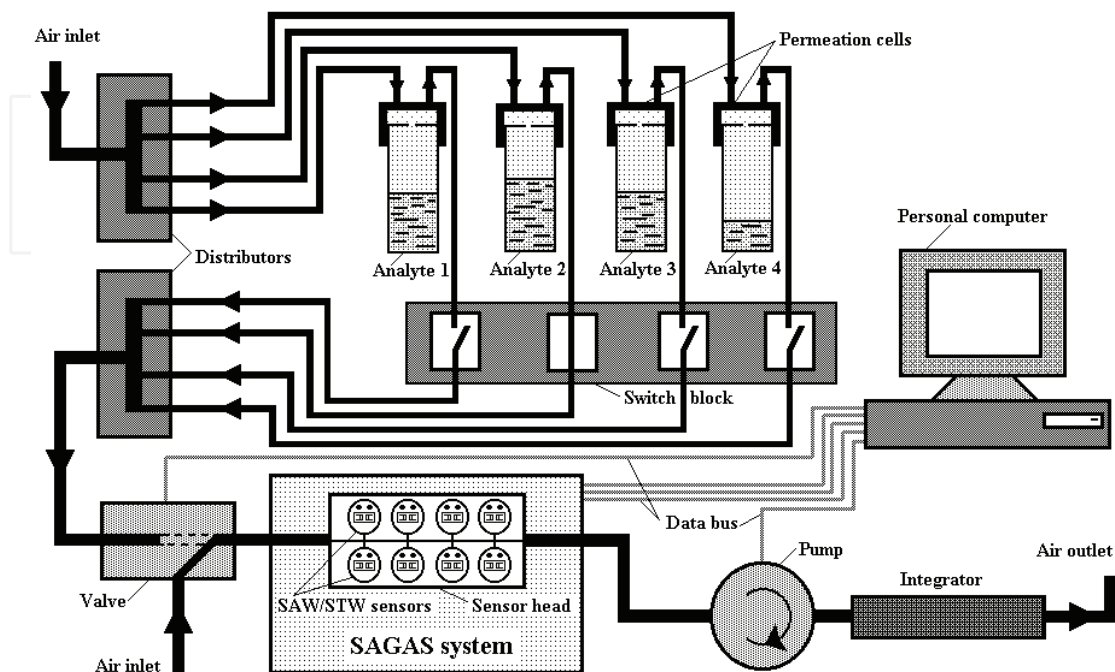

Fig. 6. Block diagram of the automated system for simultaneous gas sensitivity measurements on eight sensor devices
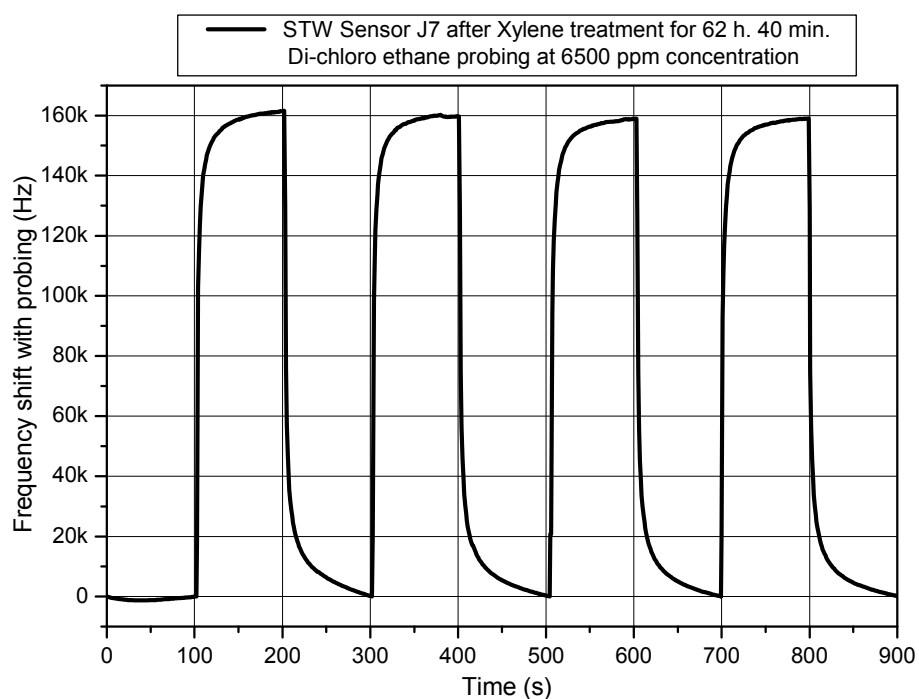

Fig. 7. Gas sensing performance of a 700 MHz styrene coated STW sensor probed with dichloroethane at 6500 ppm concentration in 100 s probe-flush cycles

7.2 Gas sensitivity comparison of RSAW/STW sensor resonators coated with solid HMDSO films

This study aims at finding out which of both acoustic wave modes provides better gas sensitivity when coated with solid HMDSO films and what is the optimum film thickness at which maximum sensitivity is achieved. For this purpose, 5 pairs of RSAW/STW devices according to Table 1 were coated at 5 different HMDSO thicknesses (50, 100, 190, 280 and 350 nm) each, in the same plasma deposition process for each pair. Figure 8 compares the gas sensing characteristics of both modes gas probed with tetrachloroethilene at 2650 ppm concentration. The results from all gas probing experiments on the 5 pairs of devices are summarized in Table 2. In this table the "sensitivity factor" is the ratio between the relative sensitivities (in ppm) for the two devices of each pair. It is given for each of the 5 film thicknesses and shows which mode is more sensitive and at which thickness. From the data in Fig. 8 and Table 2 the following important practical conclusions can be drawn:

1. *The HMDSO coated sensors have very short response times and reach adsorption-desorbtion equilibrium just a few seconds after the gas flow is applied. We attribute this behavior to the surface sorption of the HMDSO which is typical for solid sensing polymers.*

Sensor/Compound	Dichloroethane 6500 ppm	Ethylacetate 17600 ppm	Tetrachloroethylene 2650 ppm	Xylene 1400 ppm
700 MHz STW 50 nm HMDSO	2 KHz (2.9 ppm)	2.8 KHz (4 ppm)	3.5 KHz (5 ppm)	2.4 KHz (3.4 ppm)
433 MHz RSAW 50 nm HMDSO	1.5 KHz (3.5 ppm)	4 KHz (9.2 ppm)	3 KHz (6.9 ppm)	2.2 KHz (5 ppm)
Sensitivity factor (STW/ RSAW)	0.82	0.43	0.72	0.68
700 MHz STW 190 nm HMDSO	3 KHz (4.3 ppm)	4.8 KHz (6.9 ppm)	7.5 KHz (10.7 ppm)	3.7 KHz (5.3 ppm)
433 MHz SAW 190 nm HMDSO	1.8 KHz (4.2 ppm)	3.8 KHz (8.8 ppm)	3.5 KHz (8.1 ppm)	2.5 KHz (5.8 ppm)
Sensitivity factor (STW/RSAW)	**1.02**	0.78	**1.32**	0.91
700 MHz STW 280 nm HMDSO	8.3 KHz (11.9 ppm)	8.5 KHz (12.1 ppm)	7 KHz (10 ppm)	4 KHz (5.7 ppm)
433 MHz SAW 280 nm HMDSO	3.5 KHz (8 ppm)	6.5 KHz (15 ppm)	6 KHz (14 ppm)	4.3 KHz (10 ppm)
Sensitivity factor (НПАВ/RSAW)	**1.49**	0.81	0.71	0.57
700 MHz STW 350 nm HMDSO	11 KHz (15.7 ppm)	14 KHz (20 ppm)	15 KHz (21.4 ppm)	9.5 KHz (13.6 ppm)
433 MHz SAW 350 nm HMDSO	1.8 KHz (4.2 ppm)	2.3 KHz (5.3 ppm)	5.1 KHz (11.8 ppm)	4.2 KHz (9.7 ppm)
Sensitivity factor (STW/RSAW)	**3.74**	**3.77**	**1.81**	**1.4**
700 MHz STW 100 nm HMDSO	11 KHz (16 ppm)	20 KHz (29 ppm)	**37 KHz (53 ppm)**	9 KHz (13 ppm)

Table 2. Gas sensitivity comparison of RSAW vs. STW devices coated with solid HMDSO film of 5 film thicknesses. Data on the 100 nm coated SAW device are not available

Compound Concentration	Dichloroethane 6500 ppm	Ethylacetate 17600 ppm	Tetrachloroethylene 2650 ppm	Xylene 1400 ppm
700 MHz STW, 100 nm HMDSO	11 KHz (16 ppm)	20 KHz (29 ppm)	37 KHz (53 ppm)	9 KHz (13 ppm)
433 MHz RSAW, 280 nm HMDSO	3.5 KHz (8 ppm)	6.5 KHz (15 ppm)	6 KHz (14 ppm)	4.3 KHz (10 ppm)
Sensitivity factor	*STW/RSAW 2.0*	*STW/RSAW 1.93*	*STW/RSAW 3.79*	*STW/RSAW 1.3*

Table 3. Gas sensitivity comparison of the RSAW and STW sensors coated at their optimum HMDSO thickness values
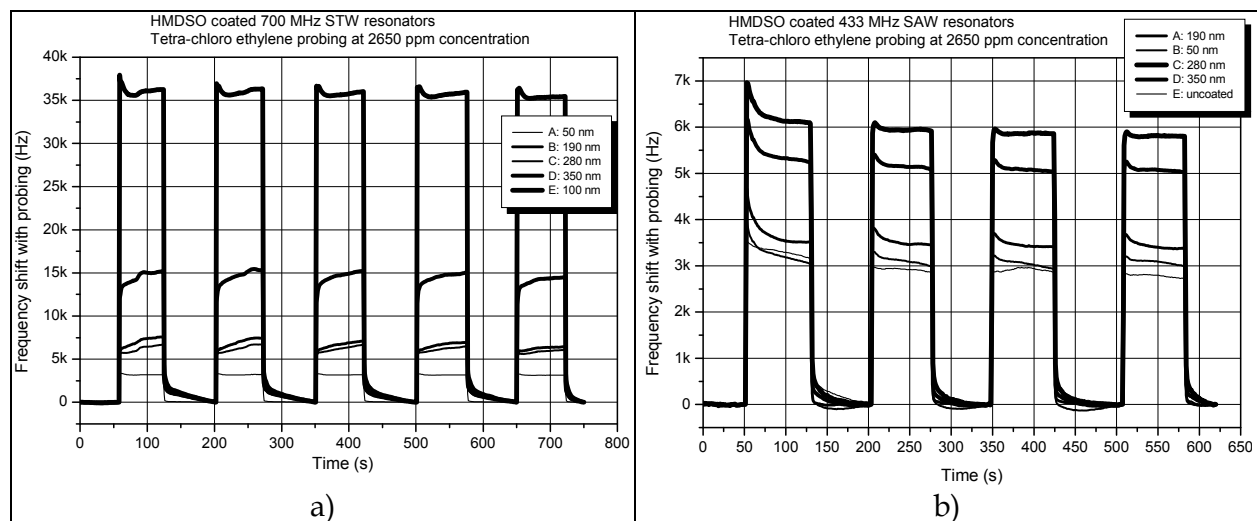
Fig. 8. Tetrachloroethilene probing data of HMDSO coated a) STW and b) RSAW sensors at 50, 100, 190, 280 and 350 nm film thicknesses

2. *Starting from very thin films (50 nm in this case) and increasing the thickness, the gas sensitivity increases in both the RSAW and STW devices, accordingly, until a thickness value is reached at which maximum sensitivity is achieved. This optimum thickness value is different for both modes (100 nm for the STW and 280 nm for the RSAW mode at the wavelength of 7,22 μm in this case). Further increase in film thickness beyond the optimum thickness value only reduces the relative frequency sensitivity and increases the loss of the gas sensor.*

3. *The optimum thickness values for both modes are far below critical thickness and are well within the thickness ranges in which the sensor devices demonstrate high mass sensitivity while retaining low insertion loss, high Q and a well behaved single-mode resonance in the Parylene C coating experiment from Fig. 5. Therefore, the practical film thickness optimization method described in Section 6 is well suited for identifying the optimum film thickness at which maximum gas sensitivity should be expected.*

4. *The relative sensitivities for both acoustic wave modes at their optimum thickness values, summarized in Table 3, demonstrate a 1,3 to 3,8 times higher sensitivity to all 4 gases of the STW mode versus its RSAW counterpart operating at the same acoustic wavelength. This suggests that the STW mode is much more appropriate for operation with solid chemo sensitive polymers.*

7.3 Gas sensitivity comparison of RSAW/STW sensor resonators coated with semisolid styrene (ST) and allylalcohol (AA) films

A similar comparative study was performed also when pairs of RSAW/STW devices from Table 1 were coated at three different thicknesses of the semisolid ST and AA polymer films in a glow discharge plasma reactor. Since no equipment was available to measure the thickness of semisolid layers directly we used the deposition time in seconds for each layer as a measure of the layer thickness. In this study the deposition times for all three thicknesses were 10, 15 and 20 s for the films with the lowest, medium and highest thicknesses, accordingly. The results from these gas probing tests are summarized in Tables 4 and 5 for the ST and AA coated sensors, accordingly. Note that in these experiments we had to reduce the concentrations of all four probing gases by a factor of 4 to avoid saturation of the sensing layers due to the much higher adsorption capacity of the ST and AA films compared to HDMSO. When comparing the data from Tables 4 and 5 an interesting behavior is observed. Styrene coated STW devices are up to 3 times more sensitive than their ST coated RSAW counterparts while with the AA coated sensors we see the opposite behavior - the AA coated RSAW devices are up to 3,6 times more sensitive than their AA coated STW counterparts. We attribute this behavior to the fact that AA is the softest of the three polymers we used in this work and this material behaves much more like a soft polymer than a semisolid one. This implies that the RSAW mode might be more suitable for operation with soft sensing films than the STW mode.

Compound/ Concentration	Tetrachloroethylene (630 ppm)		Dichloroethane (1550 ppm)		Ethylacetate (4190 ppm)		Xylene (330 ppm)	
Acoustic mode	STW	RSAW	STW	RSAW	STW	RSAW	STW	RSAW
Deposition time 10 s/styrene	119 ppm	74 ppm	100 ppm	92 ppm	94 ppm	76 ppm	71 ppm	44 ppm
Deposition time 15 s/styrene	254 ppm	85 ppm	206 ppm	171 ppm	190 ppm	95 ppm	140 ppm	65 ppm
Deposition time 20 s/styrene	239 ppm	108 ppm	219 ppm	201 ppm	206 ppm	122 ppm	111 ppm	76 ppm
Sensitivity factor 10s / 15s / 20s	*STW/RSAW 1.61 / 3.0 / 2.21*		*STW/RSAW 1.09 / 1.2 / 1.09*		*STW/RSAW 1.24 / 2.0 / 1.69*		*STW/RSAW 1.61 / 2.15 / 1.46*	

Table 4. Gas sensitivity comparison of semisolid ST coated RSAW and STW devices

Compound/ Concentration	Tetrachloroethylene (630 ppm)		Dichloroethane (1550 ppm)		Ethylacetate (4190 ppm)		Xylene (330 ppm)	
Acoustic mode	STW	RSAW	STW	RSAW	STW	RSAW	STW	RSAW
Deposition time 20 s/AA	12.3 ppm	20.8 ppm	22.8 ppm	66.4 ppm	32.6 ppm	69.9 ppm	7.1 ppm	25.2 ppm
Deposition time 25 s/AA	14.3 ppm	25.9 ppm	23.1 ppm	83.1 ppm	31.5 ppm	90.5 ppm	8.3 ppm	28.4 ppm
Sensitivity factor 20s / 25s	*RSAW/STW 1.69 / 1.81*		*RSAW/STW 2.91 / 3.18*		*RSAW/STW 2.14 / 2.87*		*RSAW/STW 3.55 / 3.42*	

Table 5. Gas sensitivity comparison of semisolid AA coated RSAW and STW devices

For the semisolid film coated RSAW/STW sensors we can make the following conclusions:

1. *Semisolid sensing films improve gas sensitivity of the RSAW and STW modes dramatically compared to the solid films. ST coated devices demonstrate one to two orders of magnitude higher relative gas sensitivities compared to HMDSO coated ones.*

2. *As observed with the solid film, also semisolid layers seem to have an optimum film thickness at which maximum gas sensitivity is achieved. Here these optimum thicknesses are achieved at 15 s for ST and 20 s for AA with the STW mode, while the RSAW mode needs somewhat higher optimum thicknesses – 20 s for ST and 25 s for the AA film.*

3. *There is a significant film type dependent difference in gas sensitivities for both modes. ST provides much better gas sensitivity compared to AA and this is attributed to both – the different sorption properties and different viscoelastic properties of the films which determine how the wave interacts with the film and the gas sorbed in it.*

4. *The RSAW mode operates better with the relatively soft AA than with the semisolid ST.*

8. Noise and measurement resolution (detection limit) of RSAW/STW resonant sensors operating with gas sensing polymer layers

As shown in Section 3, if the sensor resonator is connected in the feedback loop of a sensor oscillator whose short-term stability over the time τ has been measured as $\sigma_y(\tau)$, then measuring the sensor signal Δf which is the response of the sensor oscillator to the gas with the concentration C, the measurement resolution R, also called detection limit of the sensor system, can readily be calculated with Equation (1). As an example, let us determine the measurement resolution of the sensor system with which the dichloroethane measurement at C=6500 ppm ($6,5 \times 10^{-3}$) from Fig. 7 was performed. With $\sigma_y(\tau)$ measured as $1,17 \times 10^{-9}$/s at the oscillator frequency f_0=700 MHz (7×10^8 Hz), for the sensor resolution over the measurement time τ=1 s we obtain R=33,3 ppb (parts per billion). This means that this sensor system can detect changes in the dichloroethane concentration as small as 33 ppb. Such high sensor resolutions are extremely difficult to achieve with other sensor technologies. They are attributed to the fact that RSAW/STW resonant sensors retain excellent resonance characteristics, low loss, high Q and low flicker phase noise when coated with solid and semisolid chemo sensitive polymer films at optimum thickness.

The data in Tables 6 and 7 represent the detection limits of the styrene coated RSAW and STW sensors, respectively, during the measurements on the 4 gas-phase analytes used in this work. The $\sigma_y(\tau)$ values for the sensor oscillators were measured as $5,6 \times 10^{-9}$/s and $3,04 \times 10^{-9}$/s, respectively. The "Resolution factor" in Table 7 indicates the resolution improvement of the STW mode versus its RSAW counterpart in these measurements. In

Compound/ Concentration	Tetrachloroethylene (630 ppm)	Dichloroethane (1550 ppm)	Ethylacetate (4190 ppm)	Xylene (330 ppm)
Acoustic mode/f_0	RSAW/433 MHz			
Dep. time/polymer	20 s/styrene			
Sensor signal Δf	47 KHz (108 ppm)	87 KHz (201 ppm)	53 KHz (122 ppm)	33 KHz (76 ppm)
$\sigma_y(1s)$	$5,6 \times 10^{-9}$/s			
Resolution R	32,5 ppb	43,2 ppb	192 ppb	24 ppb

Table 6. Detection limits of the styrene coated RSAW sensors at the 4 gas-phase analytes

Compound/ Concentration	Tetra-chloro ethylene (630 ppm)	Di-chloro ethane (1550 ppm)	Ethyl acetate (4190 ppm)	Xylene (330 ppm)
Acoustic mode/fo	STW/700 MHz			
Dep. time/polymer	15 s/styrene			
Sensor signal Δf	178 KHz (254 ppm)	144 KHz (206 ppm)	133 KHz (190 ppm)	98 KHz (140 ppm)
$\sigma_y(1s)$	$3,04\times10^{-9}$/s			
Resolution R	7,5 ppb	22,9 ppb	67 ppb	7,2 ppb
Resolution factor (STW/RSAW)$^{-1}$	4,3	1,9	2,9	3,3

Table 7. Detection limits of the styrene coated STW sensors at the 4 gas-phase analytes

Table 7 this resolution improvement is by a factor of 1,9 to 4,3. We attribute this advantage of the STW mode to the following factors:

- *The styrene coated STW sensors feature lower flicker noise values than their RSAW counterparts. This is evident from the $\sigma_y(\tau)$ measurement ($5,6x10^{-9}$/s vs. $3,04x10^{-9}$/s for the RSAW and STW sensors, respectively). This suggests that the STW devices tolerate the styrene film better than the RSAW ones;*
- *The STW mode features better relative gas sensitivity than its RSAW counterpart at the same acoustic wave length and type of semisolid polymer film (styrene) as evident from Table 4.*

8.1 External factors that may degrade measurement resolution in practical RSAW/STW sensor systems

The data in Tables 6 and 7 represent the physical detection limits that can be achieved with practical RSAW/STW based sensor systems. If all other factors that may have a negative effect on the measurements are excluded then the only limiting quantity to the measurement resolution remains the electrical flicker phase noise of the sensor oscillator represented by its Allan's variation $\sigma_y(\tau)$. Unfortunately, in practical sensor systems there are several external factors that may seriously degrade sensor resolution and therefore care should be taken to eliminate them or to reduce their influence to acceptable values. The closer the system is brought to its $\sigma_y(\tau)$ limit, the better it has been designed.

The major factors that may degrade sensor resolution in practical sensor systems will be briefly discussed next.

a. *Gas flow homogeneity.*

This is one of the key disturbances that may seriously degrade sensor noise and should be eliminated first. If the gas flow applied to the sensor head from Fig. 6 is not homogeneous then the sensor devices will sense a variable gas concentration during the probe-flush cycles. Since the measurement cycle is much longer than the time over which inhomogeneities occur, amplitude fluctuation of the sensor signal at or close to equilibrium will occur. This situation is illustrated in Fig. 9 showing results from a tetrachloroethilene measurement with the setup from Fig. 6 when the integrators are removed. This causes a serious turbulence of the gas flow in the system which results in strong noise levels on top of the sensor signals. Even a periodicity on the noise signal is observed which is attributed to the pump rotation. Fortunately, gas flow

inhomogeneities are easily eliminated. After the integrators are placed back at the air inlet and outlet a noise free measurement similar to the one from Fig. 7 is obtained.
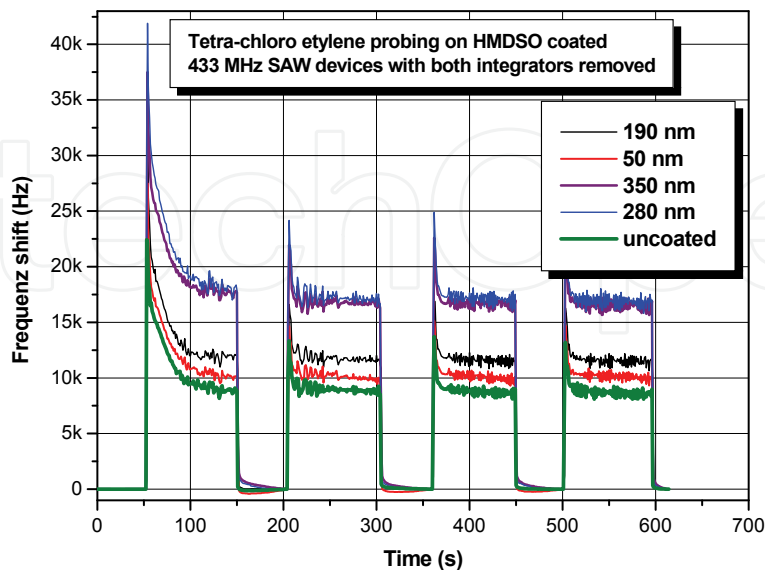

Fig. 9. Tetrachloroethilene probing with 5 HMDSO coated RSAW sensors with the integrators from the setup in Fig. 6 removed

b.   *Gas saturation of the sensing films.*
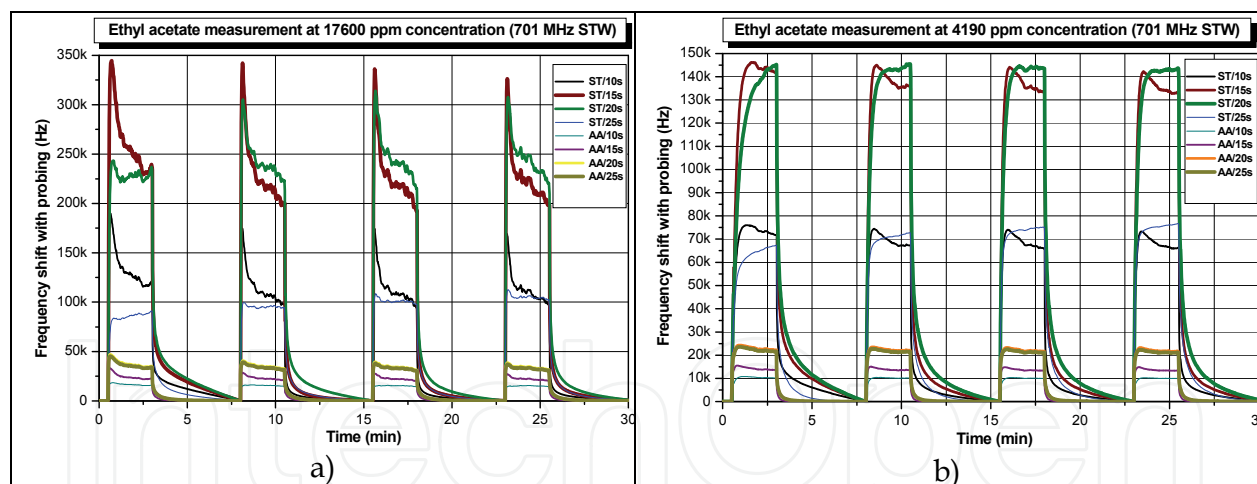
Fig. 10. Ethylacetate probing on ST and AA coated STW sensors at a) 17600 and b) 4190 ppm vapour concentration

Saturation of the sensing films occurs when gas concentrations become so high that sorption limit of the layer is reached. A situation like this during an ethylacetate measurement at 17600 ppm concentration is illustrated in Fig. 10 a). In this case strong peaks of overpressure in the analyte container as well as noise and distortion on the sensor signals are observed as a result of film saturation. When the gas concentration is reduced by a factor of 4 to 4190 ppm, the sensor signals become much more uniform and noise fluctuations are greatly reduced. The behaviour in Fig. 10 a) has the following explanation. When the films become saturated dynamic equilibrium is disturbed and a

very turbulent adsorption-desorbtion process takes place, the films get lighter and heavier in a stochastic way and this generates noise on top of the sensor signals. Once the gas concentration is reduced, equilibrium occurs and the adsorption-desorbtion process returns back to normal (see Fig. 10 b)).

c. *Adsorption-desorbtion noise (ADN) in soft film coated RSAW sensors operated far below gas saturation.*

When RSAW sensors are coated with soft polymer films featuring profound bulk sorption these films can accommodate large amounts of gas without being driven into saturation. The larger the amount of adsorbed gas, the more turbulent the adsorption-desorbtion process at equilibrium becomes even though the film is operated far below its saturation limit. This results in ADN evident in Fig. 11 which presents results from tetrachloroethilene probing on RSAW/STW sensors coated with the soft PIB film. ADN is visible on top of all sensor signals regardless of how strong they are. It should be noted that ADN levels depend entirely on the sorption characteristics of the soft polymer films and this makes elimination of this type of noise very difficult. In practical sensor systems one should either cope with ADN or, in critical situations, a different type of polymer film with lower ADN should be used. For example, the magnitude of the sensor signals in Fig. 11 is comparable with those in Fig. 7 where ST was used and no measurable ADN levels were observed. Therefore, results as the ones from the PIB film coated sensors from Fig. 11 but free of ADN could readily be obtained with ST coated sensors.
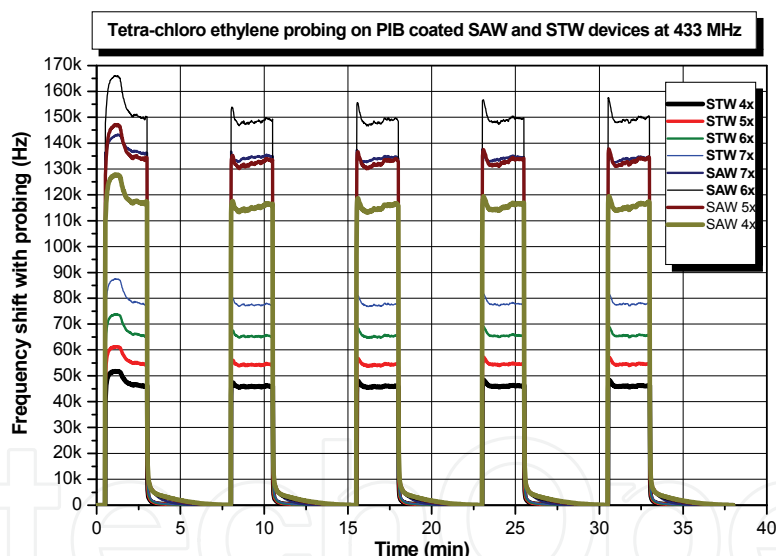
Fig. 11. Tetrachloroethilene probing on RSAW/STW sensors coated with the soft PIB polymer film and operated far below gas saturation

9. Corrosion proof RSAW resonant sensors using gold electrode structure

Typically, RSAW/STW sensors are fabricated with Al electrode structure using a well established photolithographic process. Al metallization is cheap and provides excellent electrical performance in almost all SAW devices fabricated to date. However, a major problem occurs if SAW devices with Al metallization are coated with sensing layers and used as gas sensors. Very often, the chemical gas-phase compounds to be detected form corrosive bases and alkalis with the ambient humidity and attack the Al electrode structure

by entering into a chemical reaction with the Al film. The problem is further aggravated by the presence of the sensing layer which, by absorbing large amounts of gas, greatly increases the concentration of the aggressive analyte that comes in contact with the Al electrodes. As a result of corrosion, the sensors suffer irreversible performance degradation, provide inconsistent data and even dye within a limited number of measurement cycles. The solution to that problem is the implementation of SAW devices with corrosion proof gold (Au) metallization that can successfully stand severe corrosion attacks by chemically reactive substances. The design of RSAW sensor resonators with Au electrode structure is not so straight forward as with Al metallization. Due to the fact that Au has a 7 times higher density than Al and is much softer several side effects, such as excitation of strong SSBW modes and transverse waveguide modes occur that can cause serious loss and Q-degradation as well as distorted characteristics at the main resonance. However, by careful selection of the Au thickness and choosing proper device geometry, these side effects can be kept under control and very good resonance characteristics appropriate for gas sensor applications can be achieved [22], [23]. In the next sections we will discuss the performance of RSAW sensors with Au electrode structure intended for operation as gas sensors in highly reactive chemical environments. These sensors were designed to replace their predecessors using the problematic Al electrode structure in a practical sensor system operating at 433 MHz.

9.1 Electrical performance comparison of Au vs. Al RSAW sensor resonators

Generally two types of resonator devices are used in a practical resonator system – two-port resonators (TPR) featuring a single-mode resonance and coupled resonator filters (CRF) that have a two-pole resonance achieved with a coupling grating in the centre of the resonant cavity. As evident from Fig. 12 a) and b), the CRF devices have twice the phase slope of a TPR in their filter pass bands and generally provide better stabilization of the sensor oscillator than the TPR, especially in measurements at high gas concentrations. In a real-world sensor system, the sensor oscillator is designed to operate on the right CRF resonant mode since the left one vanishes when the device is coated with a polymer film [6]. Typically, the sensor oscillator provides stable oscillation on the right mode and never jumps onto the left one since a 180 deg. phase reversal makes oscillation impossible at that mode (see Fig. 12 b)). The frequency and group delay responses of the Al RSAW devices previously used in the sensor system are shown in Fig. 12 c) and d) while a) and b) represent the electrical performance of their Au substitutes designed in [23]. The insertion loss, Q and group delay data from these devices at resonance are compared in Table 8. Es evident from that data and also from Fig. 12 the Al and Au devices feature very similar frequency responses, insertion loss and loaded Q values and the replacement of the Al devices with their Au successors was made without any changes or adjustments of the sensor circuitry. The Au devices are slightly inferior to the Al ones in terms of loss and loaded Q. This is attributed to the loss of energy as a result of the heavy Au loading on the quartz surface.

Parameter / Device (433 MHz)	Al-CRF	Au-CRF	Al-TPR	Au-TPR
Unmatched insertion loss [dB]	6.5	10.5	6.5	7.5
Group delay (50Ω load) [μs]	4.01	3.44	3.94	2.83
Loaded Q	5450	4430	5350	3890
Unloaded Q	10400	6190	10160	6730

Table 8. Comparison of the insertion loss, Q and group delay data at resonance of the uncoated RSAW sensors with Al and Au metallization characterized in Fig. 12
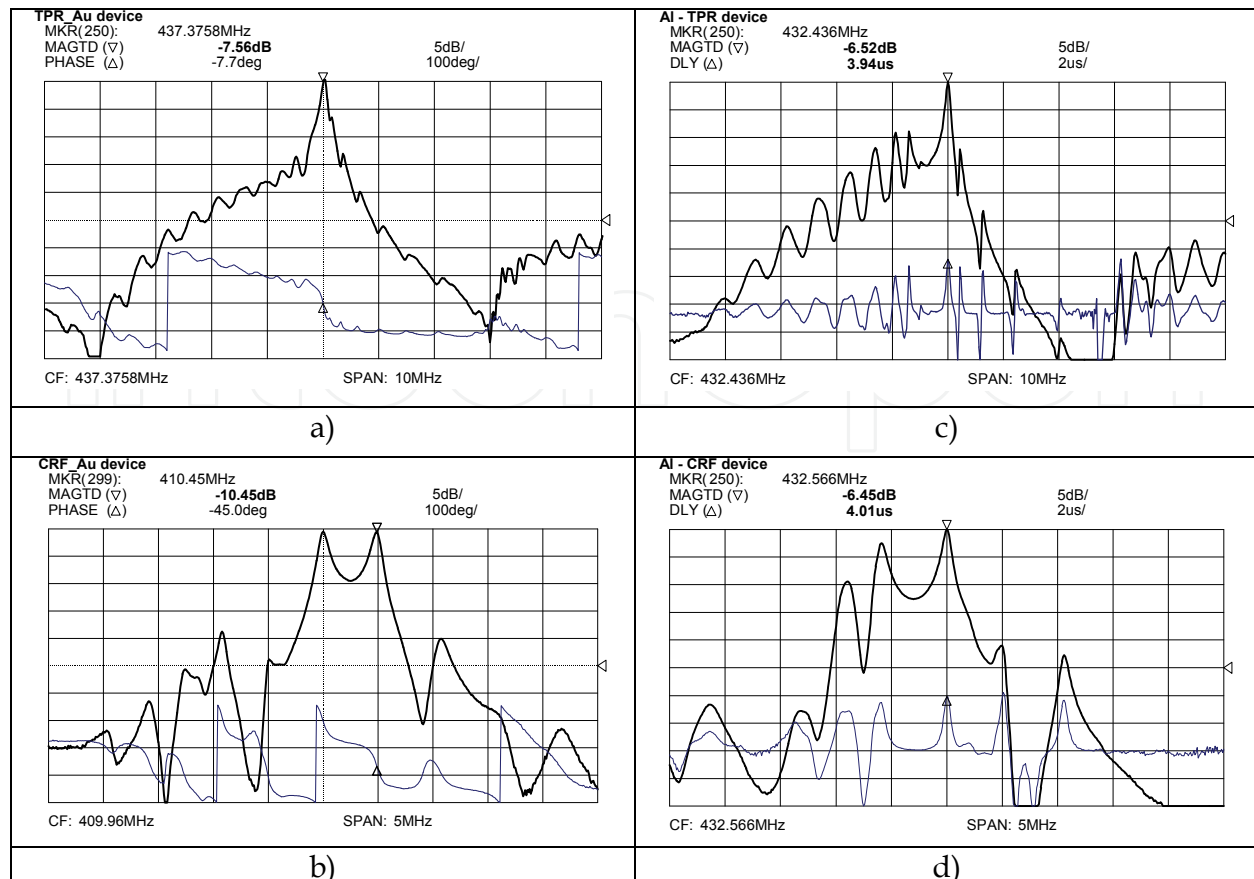
Fig. 12. Frequency (upper curves) and phase/group delay (lower curves) responses of RSAW single mode two-port resonators (upper row) and coupled resonator filter (lower row) using (a) and (b) Au and (c) and (d) Al electrode structure

9.2 Chemo sensitive polymer films and deposition methods used

This section compares the new Au vs. the old Al sensor devices in their sensor characteristics to find out if the replacement causes any performance degradation of the sensor system the Au devices were expected to operate in. To check the sensor performance we again used two types of polymer films: (A) solid Parylene C to simulate coating behaviour with solid and semisolid films as described in Section 6 and (B) a soft polymer called poly[chlorotrifluoroethylene-co-vinylidene fluoride] (PCFV) to test sensor performance at high gas concentrations. Since Parylene C coating was discussed in Section 6 already, here we will briefly discuss a relatively novel soft polymer deposition method, which is called electro spray method and is described in [24] in detail. We applied it successfully to all 4 devices from Fig. 12 to obtain very uniform high-quality soft PCFV films for reproducible sensor performance. According to this method, the holder with the SAW devices mounted on it, spins in a cloud of very small liquid-phase polymer droplets coming out from a narrow capillary tube and directed by an electrostatic field towards the sensor surface. The droplets settle onto the device surface, stick together and form a uniform film. Its thickness depends on the deposition time. Since the SAW device loss increases with film thickness, a certain insertion loss value, as necessary for optimum sensor performance, can be obtained simply by adjusting the deposition time. Except for excellent control over film thickness and uniformity [24], major advantage of this polymer coating method is that, even

at 433 MHz, the droplets are much smaller than the acoustic wavelength of about 7 μm at this frequency. Because of the small droplet size, the electro spray films cause much less propagation loss for the SAW, compared to films of the same type and thickness, deposited in an older airbrush coating technique. In contrast to electro spray films, airbrush coatings have a rough textured structure and the droplet size typically exceeds the acoustic wavelength. The two optical microscope pictures in Fig. 13 a) and b) compare the film structures of PCFV deposited with the two methods on identical 433 MHz RSAW devices. Fig. 13 a) shows part of the electrode structure and bus bars at the centre of the electro spray coated SAW device. For better visibility of the textured film structure obtained in an airbrush technique, the picture in Fig. 13 b) has been taken with a slightly higher magnification and shows part of the reflector with some free substrate area on which the large drops are clearly visible.

a)   b)
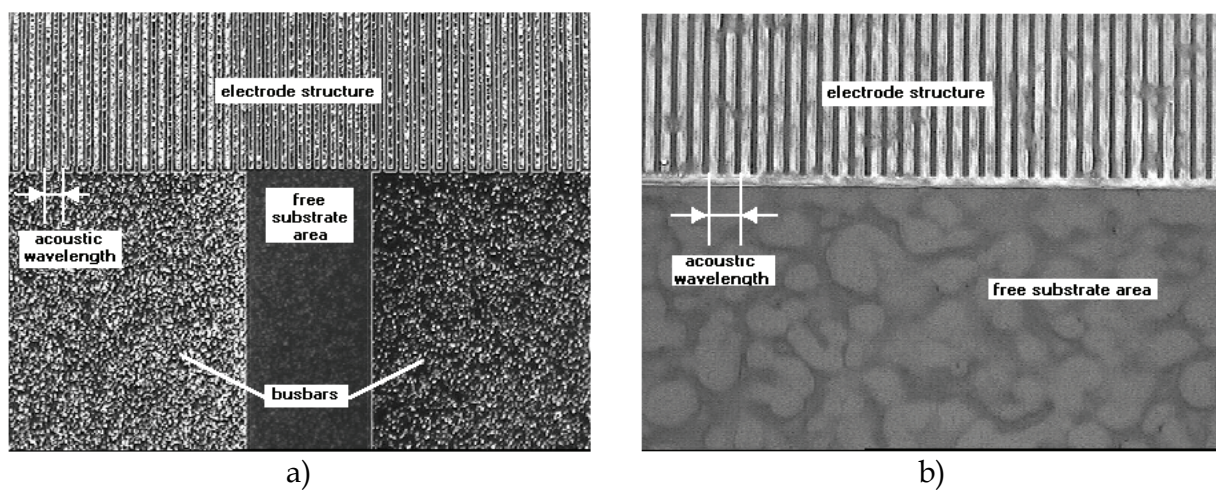
Fig. 13. Comparison of two identical RSAW devices PCFV coated with (a) the electrospray and (b) the airbrush method

9.3 Polymer coating behaviour of Au vs. Al sensor resonators

The three dimensional data plots in Fig. 14 compare the Parylene C coating behaviour of the Au and Al CRF devices from Fig. 12 b) and d) accordingly with a film thickness varying from 0 to 700 nm. In both cases the magnitude of the left longitudinal mode decreases with thickness until it disappears completely at about 300 nm for the Au and 450 nm for the Al device. Above these thickness ranges both devices demonstrate a smooth and well behaved single-mode resonance. In the 300 to 500 nm range the Au CRF reaches its highest mass sensitivity, accompanied with a gradual increase in insertion loss while the loss of the Al device decreases more rapidly. The critical for the system operation loss value of 20 dB is reached at 370 nm vs. 450 nm for the Au and Al devices, respectively.

An identical comparative Parylene C coating test, (not shown here), was performed also with the Au vs. Al TPR devices from Fig. 12 a) and c). In these tests again the Au devices were found to tolerate the solid Parylene C better than their Al counterparts. The increase in device insertion loss with Parylene C thickness for all four tested devices from Fig. 12 is shown in Fig. 15. At film thicknesses up to about 180 nm, all devices yield the same loss increase. Above 200 nm the loss behaviour starts to diverge. The two Al devices keep the same insertion loss up to about 550 nm thickness. Above 200 nm thickness, the loss of the Au devices increases at a much lower rate indicating that these devices can tolerate up to

40% thicker solid films than their Al counterparts for the same amount of loss increase. Finally, Fig. 16 compares the frequency sensitivities of the four tested devices with Parylene C film thickness which is also an indication of their gas probing sensitivity with solid films. Up to about 300 nm thickness, the sensitivity slope of the devices is nearly identical with a small advantage of the Al TPR device, followed by the Al CRF. Above 300 nm, the sensitivity slope of the Al TPR device increases but in view of its strong loss degradation, its sensitivity advantage gets lost. The other three devices keep a nearly constant sensitivity slope up to 500 nm thickness. Below the practical 370 nm thickness at which the critical for this particular system 20 dB of loss is reached for the Al devices, the sensitivity of all four devices differs by less than 20%. This difference is insignificant for practical sensor systems.
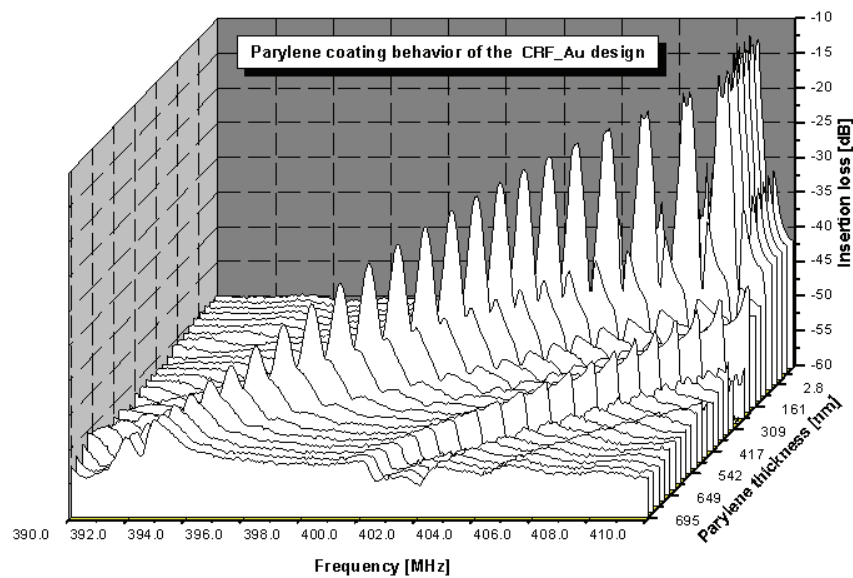
a)
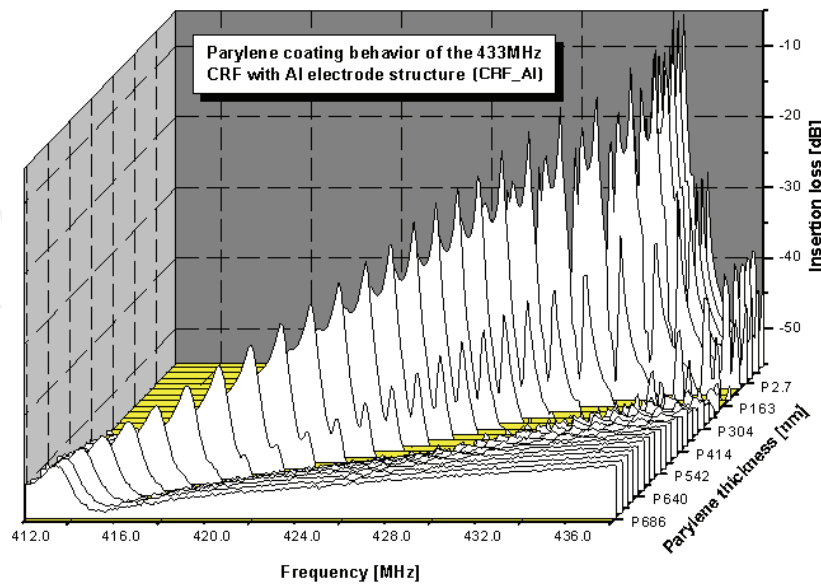
b)

Fig. 14. Parylene C coating behaviour of the RSAW CRF devices from Fig. 12 using (a) Au and (b) Al metallization
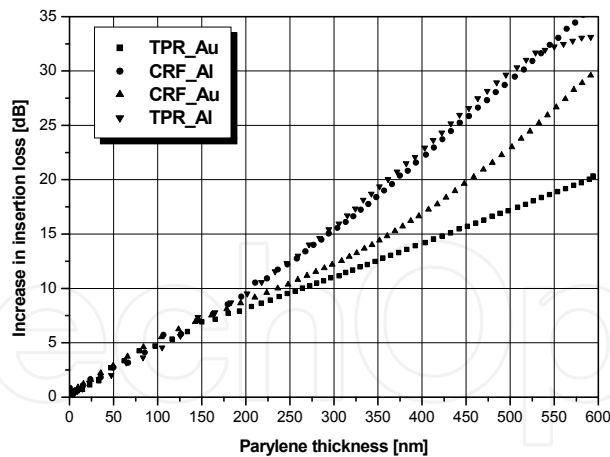
Fig. 15. Insertion loss behaviour of the Au and Al devices from Fig. 12 vs. Parylene C thickness
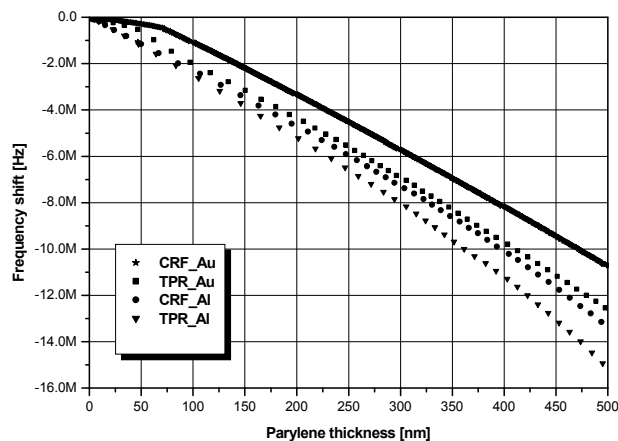
Fig. 16. Frequency (mass) sensitivity behaviour of the Au and Al devices from Fig. 12 vs. Parylene C thickness

The soft PCFV polymer coating experiments were performed on the two TPR devices from Fig. 12 a) and c) since they have about the same amount of loss prior to coating, as required by the sensor system. Since the devices are mounted on a spinning holder, monitoring of their electrical performance in the process of electro spray deposition is not possible. That is why we recorded the frequency and phase responses of each device prior to and after the deposition to obtain the frequency shift and loss increase as a function of the deposition time which we used as a measure for the thickness of the soft PCFV film. The data plots in Fig. 17 illustrate the PCFV coating behaviour of an Au TPR device in a 7,5 minutes deposition time. As a result of film loading the device loss increases by about 8 dB to 17,9 dB while its frequency shifts down by 3 MHz. The coated device on the left retains a well behaved single-mode resonance with a smooth phase response in the resonance region. The loss increase vs. thickness proportional deposition time for the Al and Au devices is shown in Fig. 18. For the Au device this dependence is linear while the Al device shows a small loss increase up to about 10 min. of deposition time and after that its loss degrades very rapidly. We attribute this behaviour again to the difference in Au vs. Al densities. Once the Au device has been optimized for operation under the heavy Au film load, it tolerates much

better the polymer film which is much lighter than Au. Finally, Fig. 19 compares the frequency sensitivity of both devices to increased PCFV thickness. The curve for the Au device is steeper meaning that its mass sensitivity is higher than its Al counterpart.
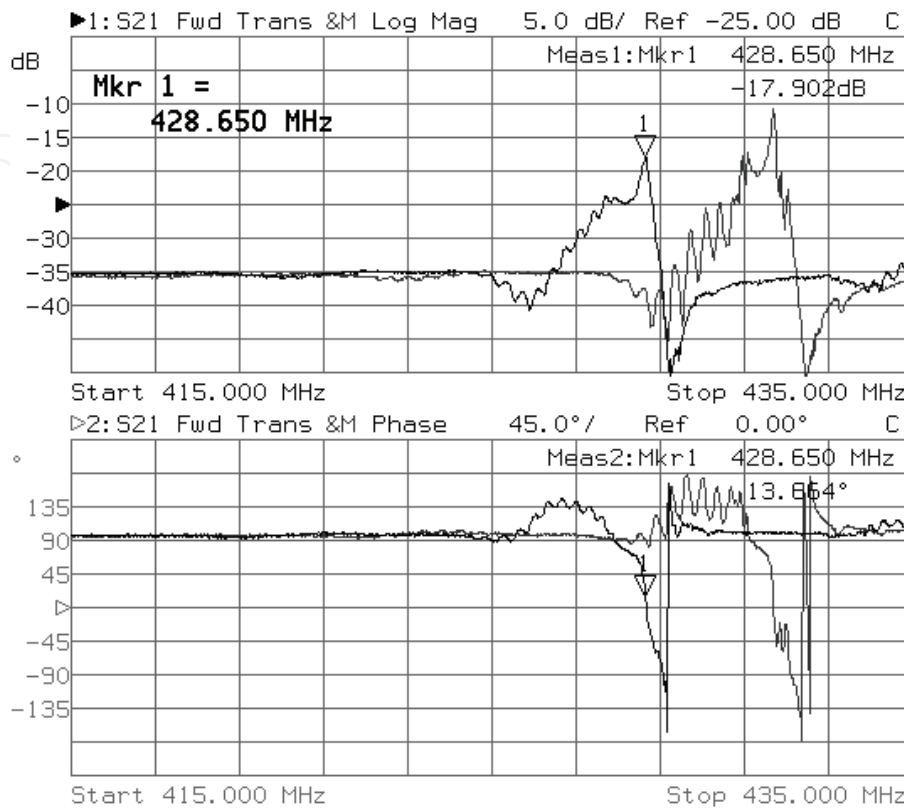

Fig. 17. Frequency responses (upper plots) and phase responses (lower plots) of an Au TPR device before (data on the right) and after (data on the left) 7.5 minutes of PCFV deposition using the electro spray method
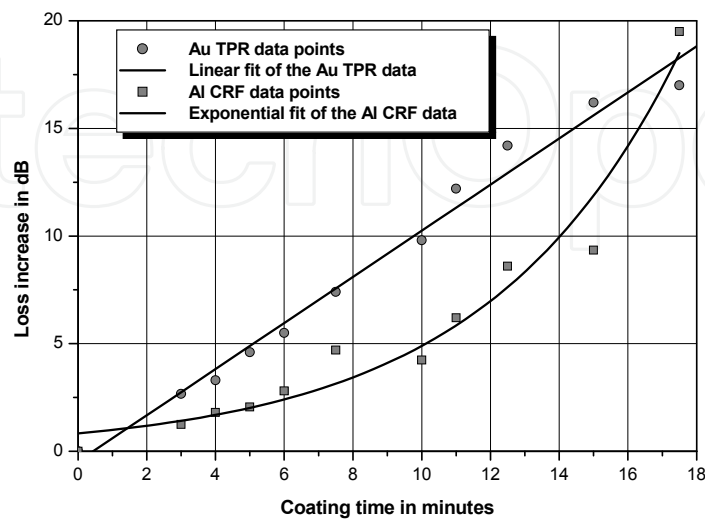

Fig. 18. Loss increase vs. deposition time for Au and Al devices electro spray coated with soft PCFV film
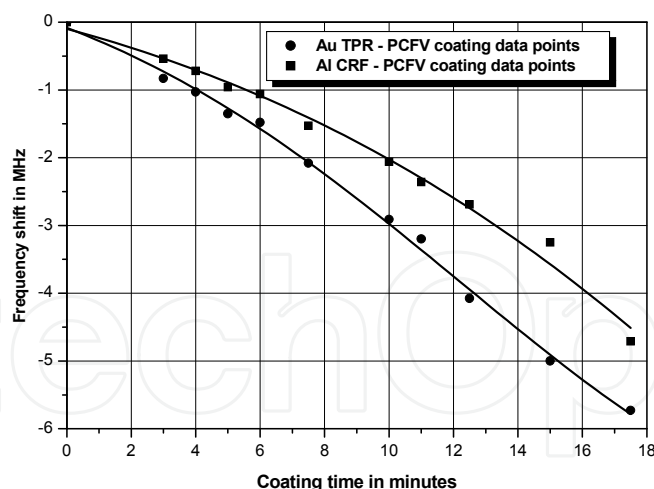
Fig. 19. Frequency downshift vs. deposition time for Au and Al devices electro spray coated with soft PCFV film

9.4 Gas probing behaviour of PCFV coated Au and Al TPR and CRF RSAW sensors

To compare the gas sensitivities of Au vs. Al sensors, pairs of devices of the same type according to Fig. 12 were PCFV coated in the same electro spray deposition method and probed with cooling agent, octane and tetrachloroethylene at different concentrations. Cooling agent and octane were among those gases that the sensors were intended to operate with in a specific application. After coating, the Au/Al pairs were selected to have nearly the same loss increase as a result of PCFV deposition to simulate identical mass loading. The gas probing results for 4 different loss increase values (thicknesses) are summarized in Table 9. As expected from the mass sensitivity data in Fig. 19, the Au devices demonstrate higher gas sensitivity than their Al counterparts. Another important conclusion evident from Table 9 is that soft polymer coating also requires an optimum film thickness for maximum gas sensitivity. In this case the optimum PCFV thickness is achieved when both the Au and Al devices are coated to about 6 dB loss increase, (numbers in bold in Table 9).

Probing gas → Loss increase values for each device pair ↓	Cooling agent 40000 ppm concentration		Octane 1100 ppm concentration		Tetrachloroethylene 1000 ppm concentration	
PCFV coated device→	Al CRF	Au TPR	Al CRF	Au TPR	Al CRF	Au TPR
Al_8/Au_8,7 dB	12,5 kHz	15 kHz	13 kHz	15 kHz	23 kHz	25 kHz
Al_6,2/Au_5,5 dB	**11 kHz**	**21 kHz**	**14 kHz**	**19 kHz**	**26 kHz**	**28 kHz**
Al_4,6/Au_4,6 dB	8 kHz	11 kHz	9 kHz	18 kHz	17 kHz	27 kHz
Al_3,5/Au_3,3 dB	6 kHz	8 kHz	11 kHz	13 kHz	17 kHz	17 kHz

Table 9. Summary of the gas probing performance of Au vs. Al device pairs PCFV coated to nearly identical loss increase values in the same electro spray deposition process

10. Summary and conclusions

This chapter has highlighted important practical aspects for the design and operation of chemical gas detection systems using STW and RSAW resonant devices. It has been shown that both acoustic wave modes provide excellent gas sensitivity and low detection limits,

down to a few ppb when coated with solid, semisolid and soft polymer sensing layers. Furthermore, the RSAW and STW modes do not only compete but rather complement each other in different measurement tasks. The STW mode operates better with solid and semisolid sensing films featuring surface sorption and is better suited for high-resolution measurements at low gas concentrations (<1%) while the RSAW mode tolerates much better thick soft sensing layers with profound bulk sorption that operate better at high gas concentrations (>1%). Carefully designed RSAW sensors with Au metallization provide an excellent corrosion proof substitute of their Al counterparts when operated in highly reactive gas-phase environments, thereby greatly increasing system reliability and measurement reproducibility over time and a large number of measurement cycles. All gas sensors, regardless of acoustic wave mode, design, metallization and type of sensing polymer requires a careful thickness optimization to provide highest gas sensitivity, maximum dynamic range and lowest detection limit.

11. Acknowledgments

12. References

[1] R. M. White, Acoustic sensors for physical, chemical and biochemical applications, *Proc. IEEE 1998 International Symposium on Frequency Control*, pp. 587-594.
[2] R. M. White, Surface acoustic wave sensors, *Proc. IEEE 1985 Ultrasonics Symposium*, pp. 490-494.
[3] H. Wohltjen, Mechanism of operation and design considerations for surface acoustic wave device vapour sensors, *Sens. Act.*, vol. 5, p. 307, 1984.
[4] R. Chung, R. A. McGill and P. Matthews, "Phase noise characterization of polymer coated SAW-gas sensors: Implications for the performance of an oscillator circuit", *Proc. 1997 IEEE Int. Freq. Control Symp.*, pp. 169-174.
[5] S. J. Martin, G. C. Frye, J. J. Spates, and M. A. Butler, Gas sensing with acoustic devices, *Proc. IEEE 1996 Ultrasonics Symposium*, pp. 423-434.
[6] M. Rapp, J. Reibel, S. Stier, A. Voigt, and J. Bahlo, SAGAS: Gas analyzing sensor systems based on surface acoustic wave devices—An issue of commercialization of SAW sensor technology, in *Proc. IEEE Int. Freq. Contr. Symp.*, 1997, pp. 129–132.
[7] E. J. Staples, Dioxin/furan detection and analysis using a SAW based electronic nose, *Proc. IEEE 1998 Ultrasonics Symposium*, pp. 521-524.
[8] E. J. Staples, T. Matsuda, and S Viswanathan, Real Time Environmental Screening of Air, Water and Soil Matrices Using a Novel Field Portable GC/SAW System, Environmental Strategies for for the 21st Century, *Asia Pacific Conference*, pp. 8-10 April 1998.

[9] United States Patent No. 5,289,715, Vapour Detection Apparatus and Method Using an Acoustic Interferometer.

[9] G. C. Frye, S. J. Martin, R. W. Cerenosek, K. B. Pfeifer, and J. S. Anderson, Portable acoustic wave sensor systems, in *Proc. IEEE Ultrason. Symp.*, 1991, pp. 311–316.

[10] G. C. Frye and S. J. Martin, Dual output acoustic wave sensor for molecular identification, in *Proc. IEEE Transducers*, 1991, pp. 566-569.

[11] T.Wessa, S. Kueppers, G. Mann, M. Rapp, and J. Reibel, "On-line monitoring of process HPLC by sensors," *Organ. Process Res. Develop.*, vol. 4, no. 2, pp. 102–106, 2000.

[12] D. A. Howe, D.W. Allan, and J. A. Barnes, Properties of Signal Sources and Measurement Methods, *U.S. Dept. Commerce, NIST Tech. Note 1337*, 1990.

[13] D. S. Ballantine, Jr. and H.Wohltjen, Elastic properties of thin polymer films investigated with surface acoustic wave devices, in *Chemical Sensors and Microinstrumentation*, R.W. Murry, R. E. Dessy,W. R. Heinemann, J. Janata, and W. R. Seitz, Eds. Washington, DC: Amer. Chem. Soc., 1989, pp. 222–236.

[14] J. W. Grate and E. T. Zellers, The fractional free volume of the sorbed vapor in modeling the viscoelastic contribution to polymer-coated surface acoustic wave vapor sensor responses, *Anal. Chem.*, vol. 72, no. 12, pp. 2861–2868, July 1, 2000.

[15] F. L. Dickert and A. Haunschild, Sensor materials for solvent vapor detection-donor-acceptor and host-guest interactions, *Adv. Mater.*, vol. 5, no. 12, pp. 887–895, Dec. 1993.

[16] N. Barie, M. Rapp, and H. J. Ache, UV crosslinked polysiloxanes as new coating materials for SAW devices with high long-term stability, *Sens. Actuators B, Chem.*, vol. B46, pp. 97–103, 1998.

[17] H. Yasuda, *Plasma Polymerization*. New York: Academic, 1985, p. 11 and 294.

[18] C. Hamann and G. Kampfrath, Glow discharge polymeric film: Preparation, structure, properties and applications, *Vacuum*, vol. 34, pp. 1053–1059, 1984.

[19] E. I. Radeva, Thin Plasma-Polymerized Layers of Hexamethyldisiloxane for Acoustoelectronic Humidity Sensors, *Sensors and Actuators*, B, vol.44, pp.275-278, 1997.

[20] G. Kovach, G. W. Lubking, M. J. Vellekoop, and A. Venema, Love waves for (bio) chemical sensing in liquids, in *Proc. IEEE Ultrason. Symp.*, 1992, pp. 281–285.

[21] I. D. Avramov, M. Rapp, A. Voigt, U. Stahl and M. Dirschka, Comparative studies on polymer coated SAW and STW resonators for chemical gas sensing applications, *Proc. 2000 IEEE International Frequency Control Symposium*, pp. 58-65.

[22] I. D. Avramov, A. Voigt and M. Rapp, "Rayleigh SAW Resonators Using Gold Electrode Structure for Gas Sensor Applications in Chemically Reactive Environments", *Electronics Letters*, 31-st March 2005, Vol. 41, No. 7, pp. 450-452.

[23] I. D. Avramov, Design of Rayleigh SAW resonators for applications as gas sensors in highly reactive chemical environments, *Proc. 2006 IEEE International Frequency Control Symposium*, 5-7 June 2006, Miami, Florida, USA, pp. 381-388.

[24] F. Bender, L. Waechter, A. Voigt and M. Rapp, Deposition of High-Quality Coatings on SAW Sensors using Electrospray, *IEEE Sensors Conference*, 2003, Paper ID 1022 (on CD).
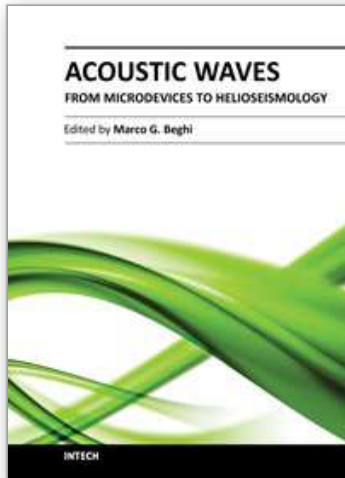
Acoustic Waves - From Microdevices to Helioseismology

Edited by Prof. Marco G. Beghi

ISBN 978-953-307-572-3

Hard cover, 652 pages

Publisher InTech

Published online 14, November, 2011

Published in print edition November, 2011

The concept of acoustic wave is a pervasive one, which emerges in any type of medium, from solids to plasmas, at length and time scales ranging from sub-micrometric layers in microdevices to seismic waves in the Sun's interior. This book presents several aspects of the active research ongoing in this field. Theoretical efforts are leading to a deeper understanding of phenomena, also in complicated environments like the solar surface boundary. Acoustic waves are a flexible probe to investigate the properties of very different systems, from thin inorganic layers to ripening cheese to biological systems. Acoustic waves are also a tool to manipulate matter, from the delicate evaporation of biomolecules to be analysed, to the phase transitions induced by intense shock waves. And a whole class of widespread microdevices, including filters and sensors, is based on the behaviour of acoustic waves propagating in thin layers. The search for better performances is driving to new materials for these devices, and to more refined tools for their analysis.

INTECH

open science | open minds